Extended Abstracts of the 2007 International Conference on Solid State Devices and Materials, Tsukuba, 2007, pp. 1182-1183

J-10-6L

Variation of Field Emission Property of Carbon Nanotube Field Emitters in Triode Structure Fabricated with Anodic Aluminum Oxide Templates

Yiming Li[1,*], Hui-Wen Cheng[1], Chen-Chun Lin[2], and Fu-Ming Pan[2]
[1]Department of Communication Engineering, National Chiao Tung University, Hsinchu, Taiwan
[2]Department of Materials Science and Engineering, National Chiao Tung University, Hsinchu, Taiwan
[*]Corresponding author. Address: 1001 Ta Hsueh Rd., Hsinchu 300, Taiwan
TEL: +886-3-5712121 ext: 52974; FAX: +886-3-5726639; and E-mail: ymli@faculty.nctu.edu.tw

1. Introduction

Carbon nanotubes (CNTs) are promising in cold-cathode flat panel displays for their chemical stability, mechanical strength, and electron emission properties [1-2]. A triode-typed field emission display (FED) possesses stable and effective emissions and high quality screen which is superior to a diode-typed one. To pursue uniform and high emission current density, it is necessary to grow vertically aligned CNT arrays on a large area with suitable tube density and tube diameters. Various template-fabrication methods have been reported [3-4]; in particular, anodic aluminum oxide (AAO) nanotemplates because AAO has vertical pore channels, highly ordered pore arrangement, and uniform pore size. Study on uniformity of FE of AAO-CNTs benefits the growth of novel structures.

In this work, new FE triode arrays with the AAO template CNTs as the field emitters are successfully fabricated and analyzed. Fabrication of AAO-CNTs is using standard integrated circuit processes in our recent work [5]. A particle-in-cell finite-difference time domain numerical simulation [6] is developed to examine the FE property in the CNT FE triode structure with the AAO template. According to our calibration, simulated data shows good agreement with the measured emission current of the AAO-CNT in the triode structure. We thus explore the effect of density and morphology of the CNTs on the uniformity of FE properties of AAO-CNT in the triode structure.

2. Fabrication and Simulation

Figure 1 shows SEM images of the fabricated samples. The AAO-CNT FE triodes are with a diameter of 7μm, the tetraethoxysilane oxide 1μm is the dielectric layer of the triode, and an Al layer 0.5μm is the gate electrode. The CNT emitters are grown in an ECR-CVD system at 600°C, and the CNTs grow along the axis of pore channels and have a tube diameter compliant with the pore size of the AAO pore channels, resulting in uniform diameter and well-aligned emitters. An Al film 2μm thick is deposited on the Si wafer, and the AAO pore channel array is subsequently prepared by electrochemical anodization in 0.3M oxalic acid solution at 21 °C under a constant polarization voltage of 40V. AAO pore channel array has highly ordered pore arrangement with a uniform pore size of 70nm~80nm and the length of the vertical pore channel is about 700nm.

With a symmetrical property of the fabricated AAO-CNTs, shown in Fig. 1(b), a two-dimensional (2D) particle-in-cell finite-difference time domain numerical simulation is developed to investigate emission current of AAO-CNT, as shown in Fig. 2. A self-consistent solution concerning the charged particles and electromagnetic (EM) field is thus obtained, as shown in Fig. 3; therefore, it includes the space charge effects automatically. As the EM fields are advanced at each time step, where the full set of Maxwell's time-dependent equations is solved for EM fields. Relative particle trajectories are solved with the Lorentz force equation. As the fields advanced at each time step, the charged particles move by following the Lorentz equation. By using the weighted charge and current density that are calculated at the grids as sources, we can advance the EM fields in the Maxwell equations. Repeating those processes for each time step until the specified setting time is reached. The emission current is computed with the Fowler-Nordheim equation shown in the inset of Fig. 4.

3. Results and Discussion

Calibration with the measured emission current density in is first performed, as shown in Fig. 4, where all settings are the same with Fig. 3. The accuracy of the 2D simulation model is justified. In the inset of Fig. 4, the parameter β increases when V_A increases. We now explore FE property due to the density and morphology of the CNT deposit. The FE property of the structure with single CNT is shown in Fig. 5. The property is sensitively affected when the number of CNTs is increased due to the screening effect, as shown in Fig. 6. The FE property is further suppressed when the number of CNTs = 30, as shown in Fig. 7. The electric field of ten CNTs is stronger than that of 30 CNTs, as shown in Figs. 6(b) and 7(b). Because high density of CNTs will have the large screening effect among adjacent emitters and reduce the magnitude of electric field, the emitted electrons attracted by anode will be fewer. The emission currents versus the number of CNTs are summarized in Tab I, where the extracted electric fields are included. The optimal FE property is examined by varying the number and the height of CNTs, as shown in Fig. 8. The emission current decreases when the number of CNTs increases for a fixed height. Similarly, for a fixed thickness of oxide and the number of CNTs, there is an optimal current versus the height of CNTs. An optimal condition on the explored AAO-CNTs is the number = 10 and the height = 0.42μm for obtaining better emission current density among others, as shown in Fig. 8. More than 1000 times difference is observed for the structure with 10 and 30 CNTs. The FE efficiency significantly depends upon the variation of height and number of CNTs. For this optimal setting, we estimate the fluctuation of FE property by randomly generated heights, as shown in Fig. 9. Taking the height of CNTs = 0.3, 0.42, and 0.46μm as the nominal cases, the currents are calculated for the statistically generated 100 heights (where 3σ = 10% variation of height is assumed) for all CNTs. The variance (the bars) of the emission current density is small for the case of height = 0.42μm, which implies that the setting has stable FE property. Effect of the diameter of CNTs is also examined, as shown in Fig. 10. Optimal diameter of CNT is about 0.04μm. For different thickness of silicon oxide, the emission current is shown in Fig. 11. For the case of thickness of oxide = 0.6μm, the FE property of triode is similar with the diode, though it has largest current.

4. Conclusions

In this study, we have explored the FE property of AAO-CNT in the triode structure. According to our calibrated model, emission current of structure has been examined with respect to different density and morphology of the CNTs. An optimal condition for growth of AAO-CNT triode structure has been found.

Acknowledgement

This work was supported in part by Taiwan National Science Council (NSC) under Contract NSC-95-2221-E-009-336, Contract NSC-95- 2752-E-009-003-PAE, by MoE ATU Program, Taiwan, under a 2006-2007 grant, and by the Chunghwa Picture Tubes under a 2006-2008 grant.

References

[1] Y. Huh *et.al*. Chemical phys. Lett. 375 (2003) 388.
[2] F. Ito *et.al*. IEEE Elec. Dev. Lett. 22 (2001) 426.
[3] J. Li *et.al*. Appl. Phys. Lett. 75 (1999) 367.
[4] P.-L. Chen *et.al*. Appl. Phys. Lett. 82 (2003) 2796.
[5] C.-C. Lin *et.al*. Diamond and Related Materials 16 (2007) 1388.
[6] K. P. Liao *et al*. J. Vac. Sci. Technol. B 25 (2007) 484.

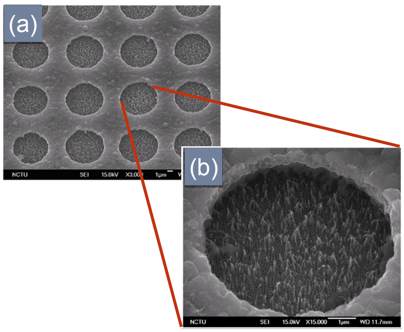

Fig. 1. (a) The SEM image of AAO-CNT triode array. (b) An enlarged plot.

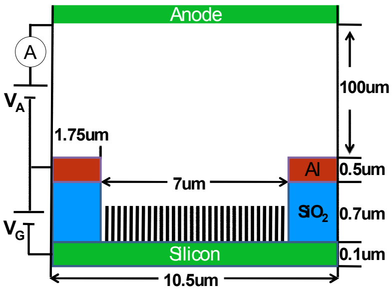

Fig. 2. A cross section view of the simulation domain of AAO-CNT triode according to a cylindrical symmetry orientation of the structure, as shown in Fig. 1(b).

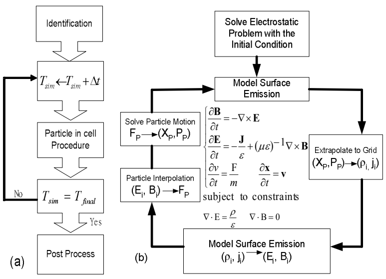

Fig. 3. (a) A computational scheme used in our 3D FDTD-PIC simulation. (b) The PIC procedure.

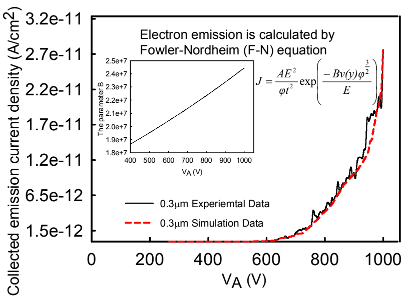

Fig. 4. Comparison between the 3D simulation and measurement of the emission current for the fabricated AAO-CNT triode. The structure is with 30 CNTs with height = 0.3μm (estimated). The inset is the calibrated parameter β versus the different applied voltage.

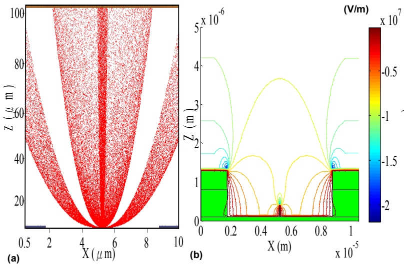

Fig. 5. The electron trajectories and electric field for the structure with single CNT, where the height of CNT is 0.42μm, V_A = 1000V and V_G = 0V.

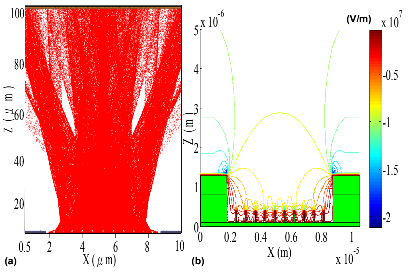

Fig. 6. The electron trajectories and electric field for the structure with ten CNTs, where the setting is the same with Fig. 5. The electric field is re-distributed due to the screening effect.

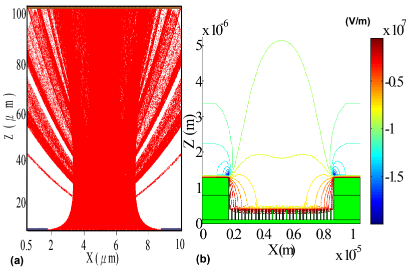

Fig. 7. The electron trajectories and electric field for the structure with 30 CNTs, where the setting is the same with Fig. 5. The strength of electric field is significantly reduced when the number of CNTs is increased, as shown in Figs. 5 and 6.

Tab. 1. Electric field and collected emission current density for the structure with 10, 15, 20, and 30 CNTs, where the setting is the same with Fig. 5. The F-N current depends upon the strength of electric field. More than 3 order magnitude difference is observed when the number of CNTs is increased from ten to 30.

Number of CNTs	10	15	20	30
E (10^6 V/m)	9.112	9.067	9.05	8.7908
I (10nA/cm^2)	63.68	6.751	1.165	0.0642

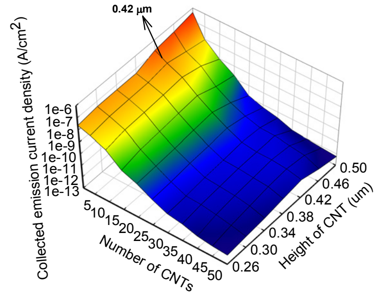

Fig. 8. The current density versus the number and height of CNTs, where V_A = 1000V and V_G = 0V.

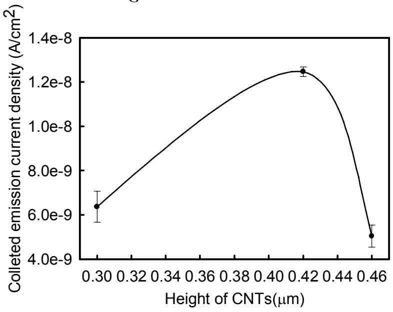

Fig. 9. The fluctuation of current density for 100 random height cases, where 3σ = 10% height, the number of CNT is 10, V_A = 1000V, and V_G = 0V.

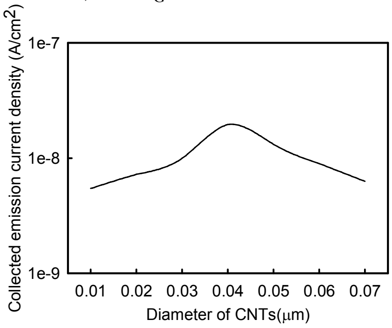

Fig. 10. The variation of current density with respect to different diameter of CNT, where the number of CNT is 10, the height of CNT is 0.42μm, V_A = 1000V, and V_G = 0V.

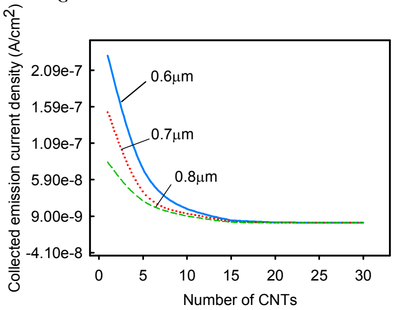

Fig. 11. The current density with respect to the thickness of oxide (SiO_2) varying from 0.6 to 0.8μm, where the height of CNT = 0.42μm, V_A = 1000V, and V_G = 0V are fixed. When the thickness of SiO_2 = 0.6μm, the structure's current attains it maximum for small number of CNTs due to the suppression of the function of gate.